Journal of Molecular Liquids 416 (2024) 126456

Contents lists available at ScienceDirect

Journal of Molecular Liquids

journal homepage: www.elsevier.com/locate/molliq

A new semi-empirical correlation for the evaluation of the dynamic viscosity of nanofluids

Gianluca Coccia *, Feliciano Falcone

Marche Polytechnic University, Department of Industrial Engineering and Mathematical Sciences, Via Brecce Bianche 12, Ancona, 60131, Italy

ARTICLE INFO

Keywords:
Nanofluid
Viscosity
Experimental
Correlation
Absolute relative deviation
n-fold cross-validation

ABSTRACT

Thanks to their excellent heat transfer coefficient, nanofluids can be considered as ideal heat transfer fluids for a large number of relevant engineering and scientific applications. Precise assessments of their thermophysical properties are thus essential for reliable calculations. In this work, a new semi-empirical scaled correlation based on 8 parameters (volume fraction, temperature, base fluid critical temperature, base fluid density, base fluid critical density, nanoparticle diameter, base fluid molar mass, nanoparticle density) is introduced to evaluate the dynamic viscosity of nanofluids. The correlation is regressed and evaluated using a dynamic viscosity dataset for 32 nanofluids, including a total of 737 experimental points: 10 nanofluids have water as base fluid (Ag, Al_2O_3, Al_2O_3/CuO, C, CuO, diamond, Fe/Si, MWCNT, ND-Ni, TiO_2), 6 nanofluids have ethylene glycol (Ag, Al2O3, CeO_2, Co_3O_4, SiC, TiO_2/CuO), 11 nanofluids comprise different mixtures of water and ethylene glycol (Al_2O_3, MWCNT/WO_3, CB, fGnP, G/Dp, G/Dr, nD87, nD97, TiO_2), 1 nanofluid has propylene glycol (SiC) and 4 nanofluids comprise different mixtures of water and propylene glycol (TiB_2, TiB_2/B_4C, fGnP). The dynamic viscosity dataset was derived from experimental measurements documented in the scientific literature and conducted with samples that were prepared using consistent and reliable methods. The study evaluates the dynamic viscosity of nanofluids using 14 literature equations to verify their accuracy against the proposed correlation. Results show that the correlation has an average absolute relative deviation of 8.16%, which is significantly lower than that of the literature equations. A 4-fold cross-validation also shows that the correlation is resilient and accurate with different regression datasets.

1. Introduction

Nanofluids are heat transfer fluids created by integrating and stabilizing nanoparticles into conventional heat transfer fluids, such as aqueous solutions, glycols, or oils. The aim is to significantly enhance heat transfer by optimizing the performance of the working fluid [1]. The study of this area can be traced back to 1881, when Maxwell developed a theoretical model for the electrical conductivity of heterogeneous systems of solid particles [2]. However, research employing micrometre- or millimetre-sized particles yielded insignificant outcomes due to the rapid settling of the particles. Furthermore, substantial concentrations of particles were necessary to attain any noticeable enhancement in fluid properties. The advent of nanotechnology in the 1980s and 1990s facilitated the acquisition of nanoparticles, which effectively addressed the issues previously identified. Nanoparticles employed in the fabrication of nanofluids can be classified into several categories, including metals, metal oxides, specialized carbon structures, and hybrid nanoparticles [3]. Their physical properties are typically more elevated than those of conventional solids. [1]. This is primarily due to their relatively high surface area to volume ratio [4].

Nanofluids can be synthesized via two distinct methods: the one-step method and the two-step method. Although the former method, which involves simultaneous mixing of the nanoparticles into the base fluid, can produce a more stable fluid in an industrial setting, the latter, which involves a step of preparing the nanoparticles as dry powders and subsequent mixing, is the preferred approach. In fact the one-step method is significantly more costly and intricate than the two-step method [5]. The maintenance of enhanced thermophysical properties in nanofluids is contingent upon the stability of the fluids. Attaining such stability frequently necessitates the implementation of two distinct methodologies: chemical and physical techniques. Chemical approaches employ the use of surfactants and pH adjustment, whereas physical approaches entail the implementation of homogenization techniques, such as ultrasound or ball milling. At present, there is no established methodology for as-

* Corresponding author.
E-mail addresses: g.coccia@staff.univpm.it (G. Coccia), f.falcone@pm.univpm.it (F. Falcone).

https://doi.org/10.1016/j.molliq.2024.126456
Received 10 September 2024; Received in revised form 1 November 2024; Accepted 5 November 2024
Available online 9 November 2024

Nomenclature

Latin Symbols

AARD	Average absolute relative deviation	%
a	Proposed correlation coefficient	
b	Proposed correlation coefficient	
c	Proposed correlation coefficient	
D	Domain of the independent variable	
d	Diameter (m), proposed correlation coefficient	
Eff	Effect size for μ_{nf}	Pa s
e	Proposed correlation coefficient	
f	Proposed correlation coefficient	
M	Molar mass	$kg\,kmol^{-1}$
N_A	Avogadro's number	$kmol^{-1}$
N	Number of experimental points	
r	Radius	m
T	Temperature	°C, K
x	Independent variable	
y	Dependent variable	

Greek Symbols

Δ	Delta difference	
η	Intrinsic viscosity	
ϕ	Volume concentration of nanoparticles	
μ	Dynamic viscosity	Pa s
ρ	Density	$kg\,m^{-3}$

Subscripts

avg	Average
bf	Base fluid
c	Critical
calc	Calculated
exp	Experimental
max	Maximum
min	Minimum
nf	Nanofluid
np	Nanoparticle

Acronyms

EG	Ethylene glycol
PG	Propylene glycol

sessing the stability of nanofluids [6]. A considerable number of studies have employed visual examination as means of assessing the stability of nanofluids. However, only a limited number of investigations have focused on the examination of more quantitative parameters such as pH and zeta potential. When the zeta potential of two particles is insufficiently high (i.e., between −25 mV and −25 mV), the particles will begin to agglomerate, leading to an unstable suspension. A high zeta potential is an effective method of preventing particle agglomeration, thereby maintaining a uniform and free-flowing dispersion [7].

Exploring the potential applications of nanofluids reveals a vast range of possibilities, which include their use in heat exchangers. In 2022, Zheng et al. [8] conducted an analysis of a double corrugated tube heat exchanger utilizing various types of water-based nanofluids. The use of H_2O+SiC (1.5% wt) resulted in a coefficient of performance of 59%, with a flow rate of 200 $L\,h^{-1}$. Focusing on the most recent results, in 2023 Ajeeb et al. [9] conducted a study on a compact exchanger utilizing Al_2O_3 nanoparticles (0.01%, 0.05%, 0.1%, 0.15%, 0.20% vol) in water and ethylene glycol mixtures. An examination of the data reveals an uptick in viscosity, reaching a maximum of 7.5% for a 0.2 vol% sample. There was a considerable improvement in thermal conductivity, which stood at 7.3% with H_2O (0.2% vol), 8.4% with EG-H_2O(80:20), and 9.1% with EG-H_2O(70:30). In the same year, Ghazanfari et al. [10] conducted an analysis of the impact of nanofluids (H_2O+Al_2O_3, 5%, 10%, 15%, and 20% vol) on the performance of a tube-and-shell exchanger. The findings indicate that while the heat transfer coefficient exhibits a 20% enhancement, the pressure drop concurrently increases by 14%.

Another area of use for nanofluids is in solar collectors, where they can be used to increase the absorption of thermal energy from solar radiation, with the aim of achieving higher operating temperatures and reducing fluid flow rates and pumping power in hydraulic circuits. In 2022, Stalin et al. [11] conducted a comparative analysis of the performance of a flat solar collector, utilizing water, the nanofluid H_2O+Fe_2O_4, and the hybrid nanofluid H_2O+Zn-Fe_2O_4. The results demonstrate that the utilization of H_2O+Zn-Fe_2O_4 (0.5% vol) enhances the thermal performance by 6.6%. The maximum energy efficiency of 80.1% is achieved at a mass flow rate of 0.1 $kg\,s^{-}1$. The hybrid nanofluid exhibited a maximum exergy efficiency of 5.36%, representing an 8.24% improvement over Fe_2O_4/water nanofluids. In the same year, Mustafa et al. [12] employed H_2O+Al_2O_3 nanofluids (0.1% vol) and H_2O+Al_2O_3-Cu hybrid (0.1% vol) in a flat solar collector. The results demonstrate that the hybrid nanofluid represents the optimal collector operating fluid, exhibiting a 4.23% increase in efficiency. Henein et al. [13] conducted an experimental analysis of the performance of an evacuated tube solar collector using the hybrid nanofluid H_2O+MgO-MWCNT. The experiments were conducted at varying weight ratios and three flow rates, ranging from 1 to 3 $L\,min^{-1}$. The results demonstrate an enhancement in the optical efficiency of the collector, reaching a maximum of 78.1%. The mean thermal power gain increased from 240 W to 495 W. The utilization of the hybrid nanofluid demonstrated an enhancement of the fluid inlet-outlet temperature differential by 56% and a reduction of the collector area by 36%.

Another promising solar collector technology is the one based on the direct absorption (DASC) of solar energy. In 2022, Balakin et al. [14] used Fe_2O_3 nanoparticles (60 nm diameter) dispersed in water, obtaining volumetric concentrations in the range of 0.5% to 2% by weight. This resulted in the formation of H_2O+Fe_2O_3, a magnetic nanofluid capable of establishing photothermal convection in an industrial-scale direct absorption solar collector equipped with a solenoid. The study yielded the highest recorded thermal efficiency of 65%. In the same year, Joseph and Thomas [15] produced a H_2O+C nanofluid using a more cost-effective one-step method. Nevertheless, a colloidal analysis revealed that the nanofluid exhibited remarkable stability for approximately six months. Subsequently, the nanofluid was employed in a DASC, with the thermal efficiency, exergy destruction, and corrosion coefficient subjected to analysis and comparison with the results obtained in the same collector using water. It was found that the thermal efficiency of the nanofluid was 73%, which is significantly higher than that of water (15%).

Fundamental thermophysical properties of nanofluids include density, specific heat, thermal conductivity, and dynamic viscosity. While simple correlations are sufficient for approximating the first two properties, this is not the case for the thermal conductivity and dynamic viscosity of nanofluids. Consequently, a considerable body of literature has emerged, comprising both theoretical and experiments studies of these transport properties. This work focuses on the dynamic viscosity of nanofluids, adopting a methodology based on previous studies [16,17]. The authors created a database of reliable experimental data to evaluate remarkable correlations of the dynamic viscosity of nanofluids. Furthermore, they advanced a semi-empirical scaled equation that, contingent on specific parameters, shows lower deviations with respect to other correlations. The primary objective is to provide engineers and scientists with a new fit-for-purpose dynamic viscosity correlation for heat transfer modeling.

The paper is organized as follows. Section 2 presents the dataset used to analyze the dynamic viscosity of nanofluids. Section 3 reviews some of the most important correlations available in the literature. Section 4 discusses the proposed semi-empirical scalad equation. Section 5 presents the literature correlations regressed on the database. Section 6 presents the findings of the analysis, including the general behavior of the equations over the entire database as well as the specific behavior for each base fluid. This section also includes a comparison between the suggested model and the literature correlations. Section 7 provides the conclusions of the work.

2. Materials and methods

This section analyzes the thermal-physical features of the studied nanofluids alongside the other relevant parameters. Regarding dynamic viscosity, this study also provides useful information on preparation methods, use of dispersants, stability assessment, and instrumentation.

2.1. Dynamic viscosity dataset of nanofluids

The dynamic viscosity dataset comprises 737 data records obtained regarding 32 nanofluids. The investigation considered five base fluids: water (H_2O), ethylene glycol (EG), propylene glycol (PG), mixtures of ethylene glycol and water (EG/H_2O), mixtures of propylene glycol and water (PG/H_2O). As regards H_2O, 10 nanoparticles (3 metal oxides, 4 metal, 3 hybrids) are found: silver (Ag), aluminum oxide (Al_2O_3), copper oxide (CuO), aluminum oxide-copper oxide (Al_2O_3-CuO), carbon (C), iron – silicon (Fe-Si), multi-walled carbon nanotube (MWCNT), nanodiamond (ND), nanodiamond-nichel (ND-Ni), titanium dioxide (TiO_2). The second base fluid (EG) comprises 6 nanoparticles (3 metal oxides, 1 metal oxides, 1 covalent compound, 1 hybrid): silver (Ag), aluminum oxide (Al_2O_3), cesium dioxide (CeO_2), cobalt trioxide (Co_3O_4), silicon carbide (SiC), titanium dioxide-copper oxide (TiO_2-CuO). Propylene glycol (PG) comprises only one type of nanoparticle, which is a covalent compound known as silicon carbide (SiC). The fourth base fluid (EG/H_2O) comprises 9 nanoparticles (4 metal, 2 metal oxides, 3 hybrid): aluminum oxide (Al_2O_3), black carbon (CB), sulfonic acid-functionalized graphene nanoplatelets (fGnP), diamond nano-mixture purified (G/D p), graphite/diamond nano-mixture raw (G/D r), nanodiamonds purified grade G01 (nD 97), nanodiamonds purified grade G (nD 87), titanium dioxide (TiO_2) and multi-walled carbon nanotube-tungsten trioxide (MWCNT-WO_3). The last base fluid (PG/H_2O) comprises 3 nanoparticles (1 metal, 1 covalent compound, 1 hybrid): sulfonic acid-functionalized graphene nanoplatelets (fGnP), titanium diboride (TiB_2), titanium diboride-boron carbide (TiB_2-B_4C).

Table 1 provides the main experimental information for the nanofluids, which includes wide ranges of dynamic viscosity, temperature, and nanoparticle concentration. Fig. 1 shows how the experimental dynamic viscosity values depend on temperature. For liquids, viscosity tends to decrease with increasing temperature. At higher temperatures, the molecules of a liquid vibrate faster and with greater intensity. This increase in kinetic energy reduces intermolecular attraction, allowing molecules to slide more easily over each other, which in turn decreases viscosity. In the following paragraphs, additional information about the experimental procedures is provided.

H_2O+Ag Khosravi-Bizhaem et al. [30] dispersed 0.2% silver by mass in water, corresponding to 0.019% by volume. The samples obtained were subjected to ultrasonication to remove any aggregation of the nanoparticles. Viscosity was measured (with an uncertainty of ±5%) at different temperatures (20-40-60 °C).

H_2O+Al_2O_3 Elcioglu et al. [31] dispersed 10 ± 5 nm and 30 ± 5 nm nanoparticles obtaining 3 different volumetric concentrations (1, 2, 3%). The stability was confirmed by measuring the zeta potential (48 mV). Nair et al. [32] prepared the nanofluid using the two-step technique by dispersing different volume concentrations, 0.5-1-1.5-2-2.5%, in water. The zeta potential was 35.1 mV and the pH was 4.3. Coccia et al. [33] dispersed different volumetric concentrations of alumina in water. The samples obtained were subjected to ultrasonication and were found stable. Nguyen et al. [34] obtained the nanofluid by dispersing particles with diameters of 36 nm and 47 nm in water, obtaining concentrations of 14-15-22% by weight. The stability was confirmed by measuring the zeta potential (47 mV).

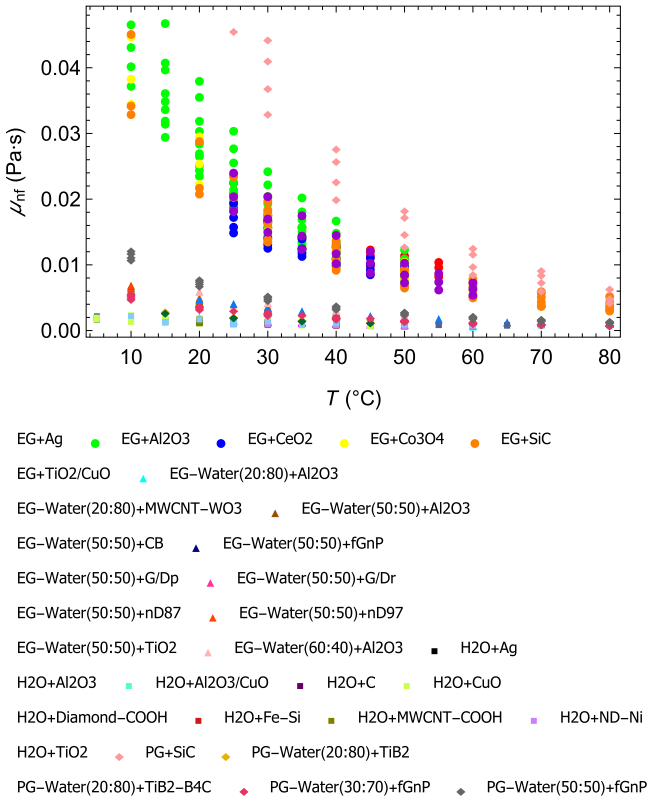

Fig. 1. Dataset experimental dynamic viscosity vs. temperature.

H_2O+Al_2O_3/CuO Zufar et al. [35] obtained this hybrid nanofluid by dispersing Al_2O_3 and CuO nanoparticles in water using the two-step method and a mixing ratio of 50:50, resulting in a weight concentration of 0.1%. The samples were then subjected to ultrasonication for 360 minutes to improve stability.

H_2O+C Dalkilic et al. [36] prepared the nanofluid by dispersing graphite nanoparticles (average diameter of 8 nm) in water and obtained four different mixtures characterized by volumetric concentrations of 0.5-1-1.5-2%. A zeta potential value of 70 mV was documented.

H_2O+CuO Nair et al. [32] prepared the nanofluid using the same method of H_20+Al_2O_3. Pastoriza-Gallego et al. [37] measured the dynamic viscosity of the nanofluid with a mass concentration in the range 1-5%. They obtained two different sets of samples. In the first, the nanoparticle had diameter between 23-37 nm. In the second the nanoparticle (d = 11 nm) was obtained according to the rapid precipitation method, proposed by Zhu et al. [47].

H_2O+Diamond Alrashed et al. [38] obtained the nanofluid by dispersing diamond nanoparticles with a diameter of 3-6 nm in water using the two-step method and without the addition of surfactants. The samples were then subjected to ultrasonication and homogenization for about 30 minutes.

H_2O+Fe-Si Huminic et al. [39] obtained the nanofluid using the two-step method. This was followed by the use of an ultrasonic disperser and a thin vibrating rod to obtain homogeneous suspensions. Three distinct suspensions (250 ml each) were prepared (mass concentration in the range 0.25-1%). The zeta potential was measured to be -72.2, -71.5 and −73.1 mV for the three different suspensions, respectively.

H_2O+MWCNT Alrashed et al. [38] used a special procedure to obtain four different volume concentrations of 0.02%, 0.08%, 0.1% and

Table 1
Dynamic viscosity experimental dataset of nanofluids.

Nanofluid	N	T_{min} °C	T_{min} °C	$\mu_{nf,min}$ Pa s	$\mu_{nf,max}$ Pa s	ϕ_{avg} %	Ref.
EG+Ag	21	25	55	0.0083	0.0226	0.50	[18]
EG+Al_2O_3	73	10	50	0.0075	0.0468	2.63	[19]
EG+CeO_2	24	25	50	0.0082	0.0195	0.22	[20]
EG+Co_3O_4	15	10	50	0.0080	0.0448	3.28	[21]
EG+SiC	44	10	80	0.0031	0.0452	0.93	[22,23]
EG+TiO_2-CuO	24	25	60	0.0055	0.0241	0.99	[24]
EG-H_2O(20:80)+Al_2O_3	25	20	60	0.0007	0.0022	0.89	[25,26]
EG-H_2O(20:80)+MWCNT-WO_3	30	25	50	0.0009	0.0018	0.29	[27]
EG-H_2O(50:50)+Al_2O_3	11	20	70	0.0011	0.0046	0.05	[28]
EGH_2OWater(50:50)+CB	16	10	80	0.0011	0.0065	0.20	[29]
EG-H_2O(50:50)+fGnP	16	10	80	0.0011	0.0066	0.18	[29]
EG-H_2O(50:50)+G/Dp	16	10	80	0.0011	0.0067	0.13	[29]
EG-H_2O(50:50)+G/Dr	16	10	80	0.0011	0.0066	0.14	[29]
EG-H_2O(50:50)+nD87	16	10	80	0.0011	0.0069	0.11	[29]
EG-H_2O(50:50)+nD97	16	10	80	0.0012	0.0070	0.11	[29]
EG-H_2O(50:50)+TiO_2	11	20	70	0.0012	0.0048	0.05	[28]
EG-H_2O(60:40)+Al_2O_3	20	20	60	0.0019	0.006	0.64	[25]
H_2O+Ag	3	20	60	0.0007	0.0013	0.02	[30]
H_2O+Al_2O_3	54	5	65	0.0006	0.0021	2.25	[31–34]
H_2O+Al_2O_3/CuO	4	50	80	0.0006	0.0007	0.02	[35]
H_2O+C	10	20	60	0.0006	0.0013	1.74	[36]
H_2O+CuO	95	5	50	0.0005	0.0023	0.92	[32,37]
H_2O+Diamond	16	20	50	0.0007	0.0011	0.11	[38]
H_2O+Fe-Si	15	20	50	0.0005	0.001	0.12	[39]
H_2O+MWCNT	13	20	50	0.0006	0.0016	0.06	[38]
H_2O+ND-Ni	8	30	60	0.0005	0.0009	0.23	[40]
H_2O+TiO_2	26	10	70	0.0007	0.0022	2.87	[41–43]
PG+SiC	24	25	80	0.0043	0.0456	0.62	[22]
PG-H_2O(20:80)+TiB_2	4	15	45	0.0013	0.003	0.46	[44]
PG-H_2O(20:80)+TiB_2-B_4C	4	15	45	0.0012	0.0027	0.71	[44]
PG-H_2O(30:70)+fGnP	35	10	80	0.0008	0.0055	0.28	[45,46]
PG-H_2O(50:50)+fGnP	32	10	80	0.0013	0.0122	0.29	[45,46]

0.2%. After dispersing the MWCNT nanoparticles (diameter 8-15 nm) in water, a magnetic stirrer was used to increase the dispersion of the nanotubes.

H_2O+ND-Ni Sundar et al. [40], prepared the hybrid nanofluid by dispersing 51.57 g and 155.56 g of ND-Ni nanoparticles in 13 L of distilled water to obtain volume concentrations of 0.1% and 0.3%, respectively. The measured diameter was 4.5 nm.

H_2O+TiO_2 Duangthongsuk and Wongwises [41] prepared the nanofluid by dispersing titanium oxide nanoparticles (diameter 21 nm) in water using the two-step method. Mixtures with volumetric concentrations of 0.2, 0.6, 1.0, 1.5 and 2.0% with pH values of 7.5, 7.1, 7.0, 6.8 and 6.5 were analyzed. Tertsinidou et al. [42] prepared the nanofluid using the same method of H_2O+Al_2O_3. Fedele et al. [43] prepared the nanofluid by sparging titanium oxide nanoparticles (diameter 40 nm) into water using the two-step method. Mixtures with volumetric concentrations of 1-10-20-35% were analyzed with pH values of 3.07, 2.34, 2.24, and 1.86, respectively. A zeta potential of 55 mV was determined for all nanofluids.

EG+Ag Zadeh and Toghraie [18] carried out the study of this nanofluid by analyzing six different volume fractions of 0.25-0.5-0.75-1-1.5-2%. The Ag nanoparticles (diameter 40 nm) were added and mixed until the nanoparticles were completely suspended, resulting in a stable colloidal mixture (ph 7 and zeta potential 50 mV).

EG+Al_2O_3 Pastoriza-Gallego et al. [19] prepared the nanofluid by dispersing alumina nanoparticles (diameter 40 nm) in ethylene glycol using the two-step method and obtained six different mixtures characterized by the volumetric concentrations 0.5, 1, 1.5, 2.1, 3.1, 4.8, and 6.6%. The pH of the solution was measured to be approximately 6-7.5.

EG+CeO_2 Saeedi et al. [20] investigated the dynamic viscosity of this nanofluid by considering six volume fractions of 0.05, 0.1, 0.2, 0.4, 0.8, and 1.2%. The nanofluid was prepared using a two-step technique to disperse nanoparticles with a diameter of 10-30 nm. The solution was first stirred for 2 hours and then ultrasonicated for 6 hours. The pH of the solution was measured to be around 6-7.5.

EG+Co_3O_4 Mariano et al. [21] prepared the nanofluid according to the two-step method, dispersing cobalt oxide nanoparticles (diameter 10-24 nm) in ethylene glycol to obtain five different mixtures with volume concentrations of 0.9, 2.1, 3.1, 4.3, and 5.7%, respectively. Stability was increased by subjecting the samples to ultrasonic cycles.

EG+SiC Akilu et al. [22] prepared the nanofluid using the two-step technique by dispersing silicon carbide nanoparticles with a diameter of 45-65 nm in ethylene glycol. Viscosity was measured at volume concentrations of 0.25, 0.5, 0.75, 1%. In the study by Colla [23], nanofluids were supplied by Nanograde Llc at concentrations of 0.1, 1 and 5% by weight. An anionic dispersant was added to the suspensions at concentrations of 0.008, 0.08, and 0.4 wt%. The reported diameter ranged from a minimum of 10 nm to a maximum of 50 nm. Dynamic viscosity was measured at room pressure and at temperatures between 10 °C and 90 °C.

EG+TiO_2-CuO Akilu et al. [24] prepared titanium-copper oxide (TiO_2-CuO) nanocomposite particles using a wet mixing protocol. The viscosity of the nanofluid was measured at various temperatures (between 303.15 K and 333.15 K) and volume concentrations (0.5, 1.0, 1.5, and 2.0%). The stability was corroborated through the measurement of the zeta potential (45 mV).

PG+SiC Akilu et al. [22] prepared and characterized the nanofluid following the same procedure for EG+SiC, again analyzing the same mass and volume concentrations.

EG-H_2O+Al_2O_3 Sundar et al. [25] synthesized the nanofluid through the dispersal of Al_2O_3 nanoparticles (average diameter 36 nm) in varying concentrations of base fluids, specifically 20:80%, 40:60%, and 60:40% by weight of ethylene glycol and water using the two-step method. Viscosity experiments were carried out at temperatures between 20 and 60 °C volume concentrations between 0.3% and 1.5%. Stability was confirmed by zeta potential analysis (39 mV). In the study

by Yiamsawas et al. [26], only the 20:80% mixture of ethylene glycol and water was used as the base fluid. Aluminum oxide nanoparticles (average diameter 120 nm) were dispersed in this mixture by the two-step method, resulting in four volumetric concentrations of 1, 2, 3, and 4%. Said et al. [28] obtained it by dispersing nanoparticles with an average diameter of 10 nm in the mixture consisting of 50:50 wt% ethylene glycol and water, giving volume concentrations of 0.05 and 0.3%. The samples were then subjected to magnetic homogenization for 30 minutes. The pH values were measured under different conditions; the mean value is approximately 8.

EG-H_2O+CB In the study by Vallejo et al. [29], carbon black (CB) nanoparticles (diameter of 13 nm) were suspended in a mixture of 50:50 wt% of ethylene glycol and water, prepared using the two-step method. To enhance the stability, the samples were subjected to ultrasonication.

EG-H_2O+fGnP The nanofluid was obtained by Vallejo et al. [29] with the same procedure as EG-H_2O+CB, using graphene nanopatterns functionalized with sulphonic acid, fGnP.

EG-H_2O+G/Dp The nanofluid was obtained by Vallejo et al. [29] with the same procedure as EG-H_2O+CB, using a purified graphite/diamond nano-mix, G/Dp, with an average diameter of 4 nm.

EG-H_2O+G/Dr The nanofluid was obtained by Vallejo et al. [29] with the same procedure as EG-H_2O+CB, using a raw graphite/diamond nano-mix, G/Dr, with an average diameter of 4 nm.

EG-H_2O+MWCNT-WO_3 In the study by Zhu et al. [27], the nanofluid was prepared using the two-step technique by dispersing nanoparticles of MWCNT (diameter 20-30 nm) and WO_3 (diameter 23-65 nm) in a mixture consisting of 20:80% by weight ethylene glycol and water. The volumetric concentrations obtained were 0.1, 0.2, 0.3, 0.4, 0.5, 0.6%. The zeta potential had a maximum value of 46.2 mV.

EG-H_2O+nD-97 The nanofluid was obtained by Vallejo et al. [29] with the same procedure as for EG-H_2O+CB, using purified nanodiamonds of grade G01, nD-97, with an average diameter of 4 nm.

EG-H_2O+nD-87 The nanofluid was prepared by Vallejo et al. [29] with the same procedure as for EG-H_2O+CB, using purified nanodiamonds of grade G, nD-87, with an average diameter of 4 nm.

EG-H_2O+TiO_2 Said et al. Said et al. [28] prepared and characterized the nanofluid following the same procedure as for EG-H_2O+Al_2O_3, using TiO_2 nanoparticles with an average diameter of 5 nm. The resulting nanofluids were then ultrasonicated. A zeta potential of −42 mV is recorded.

PG-H_2O+fGnP Vallejo et al. [45] obtained the nanofluid by dispersing sulphonic acid functionalized graphene nanopatterns (fGnP), characterized by layer heights between 2 and 18 nm and lengths and widths of approximately 530 nm, in water using the two-step method. All samples were ultrasonicated. The zeta potential was measured to be −57.1 mV. The base fluids used were mixtures of propylene glycol and water in a mixing ratio of 30:70% and 50:50% by weight. In the study by Pérez-Tavernier et al. [46], nanofluids were prepared using a mixture of propylene glycol and water in a ratio of 30:70% by weight as the base fluid. The corresponding quantities of nanoparticles were then added to obtain the desired mass concentrations of 0.25, 0.50, 0.75, and 1%. The pH was measured to be 8 and the zeta potential was approximately −48 mV for all samples.

PG-H_2O+TiB_2 Vallejo et al. [44] prepared the nanofluid by dispersing titanium diboride (diameter 1 nm) in a solution of propylene glycol and water in a proportion of 20:80% by weight using the two-step method, obtaining nanofluids with a weight concentration of 2%. The samples were then ultrasonicated for 20 minutes, to increase their stability.

PG-H_2O+TiB_2-B_4C Vallejo et al. [44] prepared and characterized the nanofluid using the same procedure as for PG-H_2O+TiB_2. The TiB_2-B_4C hybrid nanoparticles had an average diameter of about 48 nm.

Table 2
Properties of pure fluids.

Base Fluid	EG	H_2O	PG
$\Delta\mu_{bf}$ (Pa s)	0.0031-0.0335	0.0007-0.0015	0.0042-0.04
(ΔT (°C))	10-80	5-55	25-80
Ref.	[49]	[50]	[51]
$\Delta\rho_{bf}$ (kg m^{-3})	1072-1120	971.7-1005.5	990-1033
(ΔT (°C))	10-80	5-55	25-80
Ref.	[52]	[50]	[53]
M_{bf} (kg kmol^{-1})	62.07	18.01	76
Ref.	[54]	[54]	[54]
$T_{c,bf}$ (°C)	446.85	373.94	400.85
$\rho_{c,bf}$ (kg m^{-3})	360.0	400.1	338.96
Ref.	[54]	[54]	[54]

Table 3
Properties of EG-$H_2$0 mixtures.

EG-$H_2$0 (%wt)	20:80	50:50	60:40
$\Delta\mu_{bf}$ (Pa s)	0.0007-0.0016	0.0009-0.0055	0.0017-0.0054
(ΔT (°C))	20-60	10-80	20-60
Ref.	[54]	[54]	[54]
$\Delta\rho_{bf}$ (kg m^{-3})	1011.9-1029.7	1038.46-1077.5	1063.7-1086.3
(ΔT (°C))	20-60	10-80	20-60
Ref.	[54]	[54]	[54]
M_{bf} (kg kmol^{-1})	21.49	29.26	32.99
Ref.	[54]	[54]	[54]
$T_{c,bf}$ (°C)	385.17	399.86.94	405.72
$\rho_{c,bf}$ (kg m^{-3})	314.0	324.01	330.3
Ref.	[48]	[48]	[48]

2.2. Thermophysical properties of base fluids and nanoparticles

In order to evaluate the existing equations for dynamic viscosity, additional thermophysical properties of base fluids and nanoparticles was found in previous experimental works or using existing equations (with dependence on temperature): base fluid dynamic viscosity (μ_{bf}), base fluid density (ρ_{bf}), and nanoparticle density (ρ_{np}). Table 2, 3 and 4 show the ranges for the base fluid dynamic viscosity ($\Delta\mu_{bf}$), base fluid density ($\Delta\rho_{bf}$), and base fluid molecular mass (M_{bf}) within the temperatures considered, with references to data sources. In addition, the same tables show the critical temperature ($T_{c,bf}$) and the critical density ($\Delta\rho_{c,bf}$) of the base fluids considered. Table 5 presents the properties of the nanoparticles included in the database, analyzing the diameter range (Δd_{np}) and the density (ρ_{np}).

As the literature provides a limited amount of data on the density of nanoparticles, for several nanoparticles we have collected values at constant temperature, usually close to room temperature. However, given the limited effect of temperature on these properties for solid nanoparticles, we considered such constant values to be acceptable and sufficiently accurate for the present work. Many of the nanoparticle properties were extracted from the DETHERM database [48]. The density of the nanoparticles and base fluids were not only used in the proposed model (Section 4), but were also essential to calculate the volume concentration of nanoparticles (ϕ) for the references that present only mass concentrations.

3. Correlations for dynamic viscosity

Viscosity is the resistance measurement of a fluid flow between two adjoining layers. When nanoparticles are dispersed in a fluid, it can result in an augmented resistance between these layers when subjected to shear forces. This leads to an increase in the viscosity of the nanofluid.

In literature, the dynamic viscosity behavior of nanofluids has been evaluated with numerous models, both theoretical and empirical. The enhanced viscosity of nanofluids can be evaluated quantitatively using solid-fluid homogeneous equations. Unlike many review papers, which have analyzed in detail the dynamic viscosity models for nanofluids

Table 4
Properties of PG-$H_2$0 mixtures.

PG-$H_2$0 (%wt)	20:80	30:70	50:50
$\Delta\mu_{bf}$ (Pa s)	0.00011-0.0024	0.0007-0.0048	0.0011-0.0106
(ΔT (°C))	15-45	10-80	10-80
Ref.	[54]	[54]	[54]
$\Delta\rho_{bf}$ (kg m^{-3})	1007.6-1020.9	992.4-1032.5	1011.1-1048.0
(ΔT (°C))	15-45	10-80	10-80
Ref.	[54]	[54]	[54]
M_{bf} (kg kmol^{-1})	21.66	23.99	30.22
Ref.	[54]	[54]	[54]
$T_{c,bf}$ (°C)	379.33	382.00	387.42
$\rho_{c,bf}$ (kg m^{-3})	262.72	255.18	241.25
Ref.	[55]	[55]	[55]

Table 5
Properties of nanoparticles.

Nanoparticle	Δd_{np} (nm)	ρ_{np} (kg m^{-3})	T (°C)	Ref.
Ag	40-47.5	10500	20	[56]
Al_2O_3	8-68	3970	20	[57]
Al_2O_3-CuO	10	5225	25	[48]
C	8	2250	25	[48]
CB	8	1950	25	[48]
CeO_2	20	7132	20	[58]
CuO	21.5	6480	20	[48]
Diamond	4.5	3520	20	[48]
Fe-Si	200	5052	20	[39]
fGnP	210-500	2250	20	[48]
G/Dp	4	2875	20	[48]
G/Dr	4	2860	20	[48]
MWCNT	11.5	1740	25	[41]
ND-Ni	4.5	3971	20	[48]
nD87	4	3500	20	[48]
nD97	4	3520	20	[48]
SiC	55-110	3170	20	[48]
TiB_2	1	4520	25	[48]
TiO_2	5-40	4285	20	[48]
TiO_2-CuO	21.5	4702	20	[48]

available in the literature (e.g., [59–63]), this study only focuses on the analysis of the most important and simplest equations.

The pioneering model, which to this day remains the most classical [64], was derived by Einstein [65] in 1906, and is based on the assumption of a linearly viscous fluid containing suspensions of spherical particles. The model is expressed as:

$$\mu_{nf} = \mu_{bf}(1 + 2.5\,\phi) \tag{1}$$

where μ_{nf} (Pa s) is the dynamic viscosity of the nanofluid, μ_{bf} (Pa s) is the dynamic viscosity of the base fluid, and ϕ is the volume fraction of nanoparticles. Equation (1) is valid for very low volume concentrations, less than 0.02%. While many researchers have contributed to the revision of Einstein's Equation (1), it is important to note that in many of these papers, authors have typically considered inertial effects in the fluid to be negligible when assuming a very slow flow. This simplification technically imparts linearity to the equations of motion.

In 1941, Eilers [66] analyzed the viscosity of emulsions of highly viscous substances as a function of concentration. This model can be expressed as:

$$\mu_{nf} = \left(1 + \frac{1.25\,\phi}{\frac{1-\phi}{0.78}}\right)\mu_{bf} \tag{2}$$

Based on the model developed by Einstein [65], in 1945 De Bruijn [67] proposed the following model, valid for volumetric concentrations between 2 and 10%:

$$\mu_{nf} = \mu_{bf}\,(1 - 2.5\,\phi + 1.55\,\phi^2) \tag{3}$$

Vand [68] proposed his theory of the viscosity of concentrated suspensions in 1945. He stated that, if one assumes that the suspension behaves hydrodynamically with respect to an additional particle as a homogeneous medium [68], considering the effect of Brownian motion and reciprocal forces in the suspension, it is possible to derive a model valid for concentrations above 2%. Starting from Equation (1), taking into account an infinitesimal increase in viscosity dμ, an infinitesimal increase in volume dV, and integrating, it turns out that the model may be written:

$$\mu_{nf} = \mu_{bf}\left(1 - \phi - 1.16\,\phi^2\right)^{-2.5} \tag{4}$$

In 1950, Saitô [69], based on Eilers [66] equation, proposed the following model, which is valid for volumetric concentrations above 1.5%:

$$\mu_{nf} = \left(1 + \frac{2.5\,\phi}{1-\phi}\,\phi\right)\mu_{bf} \tag{5}$$

Brinkman [70] extended Einstein [65] formula to a moderate particle volume concentration up to 4%. It is expressed as:

$$\mu_{nf} = \mu_{bf}\left(\frac{1}{(1-\phi)^{2.5}}\right) \tag{6}$$

The Krieger and Dougherty [71] equation is the most widely cited model for high particle volume concentrations. The model has the following form:

$$\mu_{nf} = \mu_{bf}\left(1 - \frac{\phi}{\phi_{min}}\right)^{\eta\,\phi_{min}} \tag{7}$$

where ϕ_{min} represents the maximum volume concentration, typically ranging from 0.495 to 0.54 under quiescent conditions and reaching 0.605 at high shear rates. η represents the intrinsic viscosity. The typical value for mono-disperse spheres is approximately 2.5. Some researchers developed empirical models for the dynamic viscosity of particle-fluid mixtures in exponential form, considering micron-sized particles. These include the equation by [72], who proposed the following model in 1965:

$$\mu_{nf} = \mu_{bf}\left(1 + 2.5\,\phi + 10.5\,\phi^2 + 0.00273\,e^{1.66\,\phi}\right) \tag{8}$$

In 1970, Nielsen [73] proposed a generalized equation for the dynamic viscosity of composites for a 2% concentration of dispersed particles:

$$\mu_{nf} = \mu_{bf}(1 + 1.5\,\phi)e^{\frac{\phi_{min}}{1-\phi_{min}}} \tag{9}$$

where ϕ_{min} is the maximum volumetric concentration.

Alternatively, in 1972, Lundgren [74] proposed the subsequent equation as a Taylor series in ϕ:

$$\mu_{nf} = \frac{1}{1 - 2.5\,\phi}\,\mu_{bf} \cong \mu_{bf}\left(1 + 2.5\,\phi + \frac{25}{4}\,\phi^2 + O\left(\phi^3\right)\right) \tag{10}$$

The above equation is also in the form of the Einstein [65] model, if the term O(ϕ^3) or higher is neglected.

In 1977, Batchelor [75] conducted an evaluation of the impact of Brownian motion on the dynamics of anisotropic suspended systems comprising rigid, spherical particles. For suspensions with volumetric concentration values below 10%, he proposed the following model:

$$\mu_{nf} = \mu_{bf}\left(1 + 2.5\,\phi + 6.5\,\phi^2\right) \tag{11}$$

Based on Einstein [65] model and fitting the curve to the empirical data of Wang et al. [76] in 2004, Maıga et al. [77] developed the following model:

$$\mu_{nf} = \mu_{bf}\,(1 + 7.3\,\phi + 123\,\phi^2) \tag{12}$$

The models described above show a tendency for viscosity to increase with volume fraction when spherical nanoparticles are considered. However, experimental data contradict this trend. Indeed, the

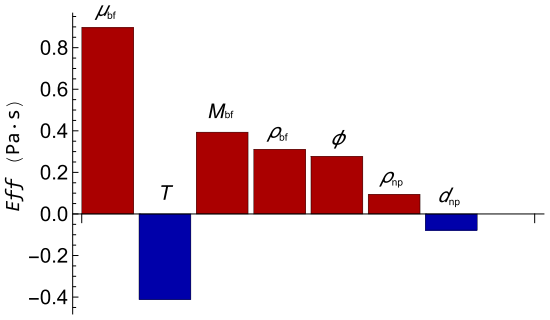

Fig. 2. Results of the effect size analysis.

dynamic viscosity of nanofluids is a thermophysical property that cannot be explained by considering only the concentration of nanoparticles dispersed in the base fluid. In fact, viscosity also depends on other parameters such as the properties of the nanoparticles, the temperature, and the properties of the base fluid used.

In 2006, Guo et al. [78] stated that small particle size induces high viscosity values in nanofluids; therefore, they updated the correlation proposed by Batchelor [75] to include the effect associated with nanoparticle size (d_{np}), and proposed the following model:

$$\mu_{nf} = \mu_{bf}\left(1 + 2.5\,\phi + 6.5\,\phi^2\right)\left(1 + 350\,\frac{\phi}{d_{np}}\right) \tag{13}$$

In 2011, Corcione [79] proposed the following model to estimate the dynamic viscosity of nanofluids:

$$\mu_{nf} = \frac{\mu_{bf}}{1 - 34.87\left(\frac{d_{np}}{d_{bf}}\right)^{-0.3}\phi^{1.3}} \tag{14}$$

where d_{np} (m) is the nanoparticle diameter and d_{bf} indicates the equivalent diameter of a base fluid molecule, which can be calculated using the following equation:

$$d_{bf} = 0.1\left(\frac{6\,M_{bf}}{N_A\,\pi\,\rho_{273\,K}}\right)^{\frac{1}{3}} \tag{15}$$

where M_{bf} represents the molar mass of the base fluid, N_A is Avogadro's number, and $\rho_{273\,K}$ indicates the density of the base fluid at 273 K.

4. Proposed correlation for dynamic viscosity

A new semi-empirical equation, which takes into account the dependence of dynamic viscosity of nanofluids (μ_{nf}) on temperature, nanoparticle diameter, volumetric concentration, and the properties of the base fluid used, such as dynamic viscosity, density and molar mass, is proposed in this work. The main parameters of the equation were selected by using an effect size analysis [80–82], i.e. a statistical procedure carried out on all the experimental dataset. As demonstrated in Fig. 2, the selected parameters have unambiguous statistical impacts (effects, *Eff*) on μ_{nf}. To define the effect size *Eff* used in the present paper, let us consider an independent variable x, which can assume the values $x_i \in [x_{min}, x_{min}]$ $(i = 1, \ldots, N)$. The domain of the independent variable, D, can be subdivided into $D^+ = \{x \in D \mid x_i > (x_{min} + x_{min})/2\}$ and $D^- = \{x \in D \mid x_i < (x_{min} + x_{min})/2\}$. The effect size of x for the dependent variable $y(x)$ (i.e., μ_{nf} in this study) is defined as:

$$Eff(x) = \frac{\sum_{x\in D^+} y(x)}{\mathrm{card}\left(D^+\right)} - \frac{\sum_{x\in D^-} y(x)}{\mathrm{card}\left(D^-\right)} \tag{16}$$

where card is the cardinality of the subdomains D^+ and D^-. Based on Eq. (16), *Eff* has the same unit of measurement of μ_{nf} (Pa s).

The proposed equation is as follows:

$$\mu_{nf} = \mu_{bf}\left[1 + \left(a\,\phi^b\right)\left(\frac{T}{T_{c,bf}}\right)^c\left(\frac{\rho_{bf}}{\rho_{c,bf}}\right)^d\left(\frac{d_{np}}{2\,r_{Bohr}}\right)^e\left(\frac{M_{bf}}{N_A\,\rho_{np}\,d_{np}^3}\right)^f\right] \tag{17}$$

where μ_{bf} is the dynamic viscosity of the nanofluid (Pa s), ϕ is the volume fraction of nanoparticles, T is the temperature (K), $T_{c,bf}$ is the critical temperature of the base fluid (K), ρ_{bf} is the density of the base fluid (kg m^{-3}), $\rho_{c,bf}$ is the critical density of the base fluid (kg m^{-3}), M_{bf} is the molar mass of the base fluid (kg kmol^{-1}), N_A is Avogadro's number (kmol^{-1}), ρ_{np} is the density of nanoparticles (kg m^{-3}), and d_{np} is the average diameter of the nanoparticles (m). The term $r_{Bohr} = 5.292 \times 10^{-11}$ m is the Bohr radius. It represents the most probable distance between a hydrogen atom nucleus and its electron in its ground state. The values of the scaled regression coefficients ($a = 4.34 \times 10^{-5}$, $b = 0.55$, $c = 1$, $d = 2.61$, $e = 1.63$, $f = 0.59$) were determined using a Random Search Method (RSM) [83]. This procedure was undertaken with the objective of minimizing the average absolute relative deviation (AARD) between the values calculated from the proposed equation and the data presented in Table 1. AARD(μ_{nf}) is expressed as:

$$AARD\left(\mu_{nf}\right) = \frac{100}{N}\sum_{i=1}^{N}\left|\frac{\mu_{nf,calc} - \mu_{nf,exp}}{\mu_{nf,exp}}\right| \tag{18}$$

where N in the number of experimental points, while $\mu_{nf,calc}$ and $\mu_{nf,exp}$ are the calculated and experimental dynamic viscosity of nanofluids, respectively. It is important to note that the coefficients regressed for the selected nanofluids are applicable within the following ranges: $0.018 \le \phi \le 5.7, 5\,°C \le T \le 80\,°C, 1\,nm \le d_{np} \le 500\,nm, 971.71\,kg\,m^{-3} \le \rho_{bf} \le 1120.23\,kg\,m^{-3}$.

5. Literature equations regressed on the database

Using the Random Search Method (RSM) [83], the literature equations were regressed using the collected dataset of thermophysical properties. The aim of this procedure was to determine new coefficients that, when applied to the equations, would enhance the predictions of the dynamic viscosity of nanofluids.

Table 6 shows the results of this operation. The second column includes the reference to the original equation (Section 3), while the third column shows the equation with the new regression coefficients obtained.

6. Results and discussions

This section presents a comprehensive analysis of the results obtained with several equations selected from the literature (Section 3). Subsequently, the results obtained with the suggested scaled equation (Section 4) are presented and analyzed in comparison with the literature equations. Lastly, the results derived from the literature equations regressed on the proposed database (Section 5) are provided.

6.1. Literature equation results

The AARD of the 14 selected literature equations were analyzed using the recorded experimental dataset (Table 1). The result of the analysis is provided in Table 7, which shows the percentage AARD(μ_{nf}) values provided by these equations for all listed nanofluids. Table 7 shows that Maiga's equation (12) has the smallest deviation between the calculated μ_{nf} and the experimental values, with an average AARD of 12.33%. Guo's model (13), on the other hand, is identified as the weakest model available in the literature, with an average AARD of 23.09%. The models proposed by Einstein (1), Vand (4), Brinkman (6) and Thomas (8) are almost completely equivalent, with an average AARD of around 13.7%. The average AARDs of the models of Saito (5), Krieger-Dougherty (7)

Table 6
Results of RSM applied to the literature equations.

Model from literature	Original Eq.	Regressed equation
Einstein [65]	(1)	$\mu_{nf} = \mu_{bf}\,(1 + 14.41\,\phi)$
Eilers [66]	(2)	$\mu_{nf} = \left(1 + \frac{19.34\,\phi}{\frac{1-\phi}{0.71}}\right)\mu_{bf}$
De Bruijn [67]	(3)	$\mu_{nf} = \mu_{bf}\,(1 + 21.87\,\phi - 276.65\,\phi^2)$
Vand [68]	(4)	$\mu_{nf} = \mu_{bf}\left(1 - \phi - (-12.80)\,\phi^2\right)^{-19.04}$
Saitô [69]	(5)	$\mu_{nf} = \left(1 + \frac{205.74\,\phi}{1-\phi}\phi\right)\mu_{bf}$
Brinkman [70]	(6)	$\mu_{nf} = \mu_{bf}\frac{1}{(1-\phi)^{1.2}}$
Krieger and Dougherty [71]	(7)	$\mu_{nf} = \mu_{bf}\left(1 - \frac{\phi}{-0.0029}\right)^{2.43\,\phi_{min}}$
Thomas [72]	(8)	$\mu_{nf} = \mu_{bf}(1 + 8.34\,\phi - 47.73\,\phi^2 + 0.08\,e^{14.61\phi})$
Nielsen [73]	(9)	$\mu_{nf} = \mu_{bf}(1 + 11.43\,\phi)e^{\frac{\phi_{min}}{1-\phi_{min}}}$
Lundgren [74]	(10)	$\mu_{nf} = \frac{1}{1-8.08\,\phi}\,\mu_{bf}$
Batchelor [75]	(11)	$\mu_{nf} = \mu_{bf}\left(1 + 21.87\,\phi - 276.65\,\phi^2\right)$
Maıga et al. [77]	(12)	$\mu_{nf} = \mu_{bf}\left(1 + 21.87\,\phi - 276.65\,\phi^2\right)$
Guo et al. [78]	(13)	$\mu_{nf} = \mu_{bf}\left(1 + 15.72\,\phi + 0.78\,\phi^2\right)(1 - 1.57043\,10^{-8}\,\frac{\phi}{d_{np}})$
Corcione [79]	(14)	$\mu_{nf} = \frac{\mu_{bf}}{1-0.78\left(\frac{d_{np}}{d_{bf}}\right)^{0.13}\phi^{0.4}}$

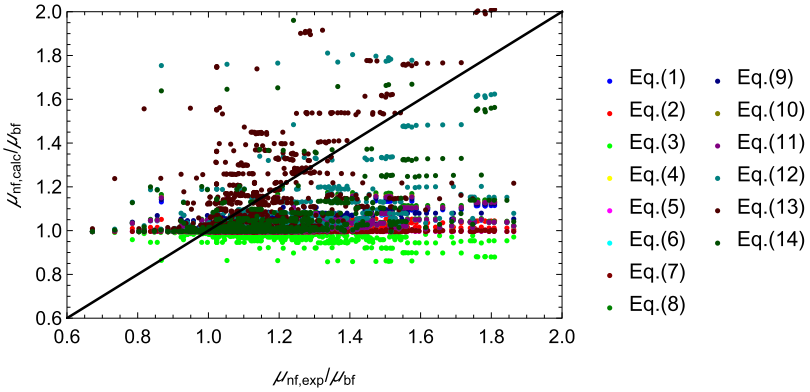

Fig. 3. Experimental reduced dynamic viscosity vs. calculated values for all equations. Some points out of the displayed range are not shown.

Table 7
Average AARD(μ_{nf}) (%) of all the literature equations.

Model	Avg. AARD(μ_{nf}) (%)	Eq.
Einstein [65]	13.80	(1)
Eilers [66]	14.43	(2)
De Bruijn [67]	16.18	(3)
Vand [68]	13.74	(4)
Saitô [69]	14.88	(5)
Brinkman [70]	13.77	(6)
Krieger and Dougherty [71]	14.86	(7)
Thomas [72]	13.59	(8)
Nielsen [73]	13.47	(9)
Lundgren [74]	13.75	(10)
Batchelor [75]	14.75	(11)
Maıga et al. [77]	12.33	(12)
Guo et al. [78]	23.09	(13)
Corcione [79]	13.29	(14))
All selected models [65–79]	14.66	(1)-(14)
Proposed model	8.16	(17)

and Eilers (2) are equivalent, averaging about 14.8%. On average, all models in the literature have an AARD of 14.66%.

Figs. 3 and 4 illustrate a comparative analysis between experimental data and calculated values for nanofluids. Fig. 3 displays the results for the literature equations, whereas Fig. 4 categorizes the base fluids. Based on Fig. 3, the literature's equations often underestimate μ_{nf}. Specifically, De Bruijin's, Krieger-Dougherty's, Thomas's, and Batchelor's models (Eqs. (3), (7), (8), and (11)) show this tendency. In contrast, Maiga and Guo's models (Eqs. (12) and (13)) tend to overestimate the dynamic viscosity calculation.

6.1.1. Results for water-based nanofluids

The analysis of the nanofluids comprising H_2O as the base fluid reveals that the optimal model is that of Lundgren (10), as depicted in Table 8, showing an average AARD(μ_{nf}) of 10.60%. Conversely, the least effective model is the one by Guo (13), displaying an average AARD of 40.87%. The model shows criticality with the following nanoparticles: Al_2O_73, C, CuO, ND-Ni, TiO_2. With the exception of Guo (13), the analysis of the data shown in Table 8 reveals that the average AARDs yielded by the different models are nearly the same (about 11%). Fig. 4(a) illustrates the tendency for equations in literature to generally underestimate μ_{nf}. It is worth noting that the distribution of points is quite symmetrical. Notably, nanofluids containing oxide nanoparticles, such as Al_2O_3 and CuO, are particularly underestimated. Conversely, the H_2O+TiO_2 nanofluid appears to be overestimated.

6.1.2. Results for ethylene glycol-based nanofluids

Analyzing in detail the nanofluids with EG as the base fluid (Table 9), it emerges that the best model is Maiga's (12), with an AARD of 13.97%; the worst model, instead, is Saito's (5), with an AARD of 24.52%. From the same table, it can be seen how this result is affected by the nanofluid EG+SiC, for which the AARD is 45.93%. Furthermore, it appears that the Krieger-Dougherty (7) and De Bruijin (3) models show an AARD greater than 20% for almost all EG-based nanofluids. Fig. 4(b) illustrates how equations in the literature typically underestimate μ_{nf}. The ethylene glycol-based nanofluids that are most underestimated include those containing Al_2O_3, Ag (at low volumetric concentrations), and SiC. On the other hand, the nanofluids EG+Ag (at high volumetric concentrations) and EG+Co_3O_4 are overestimated.

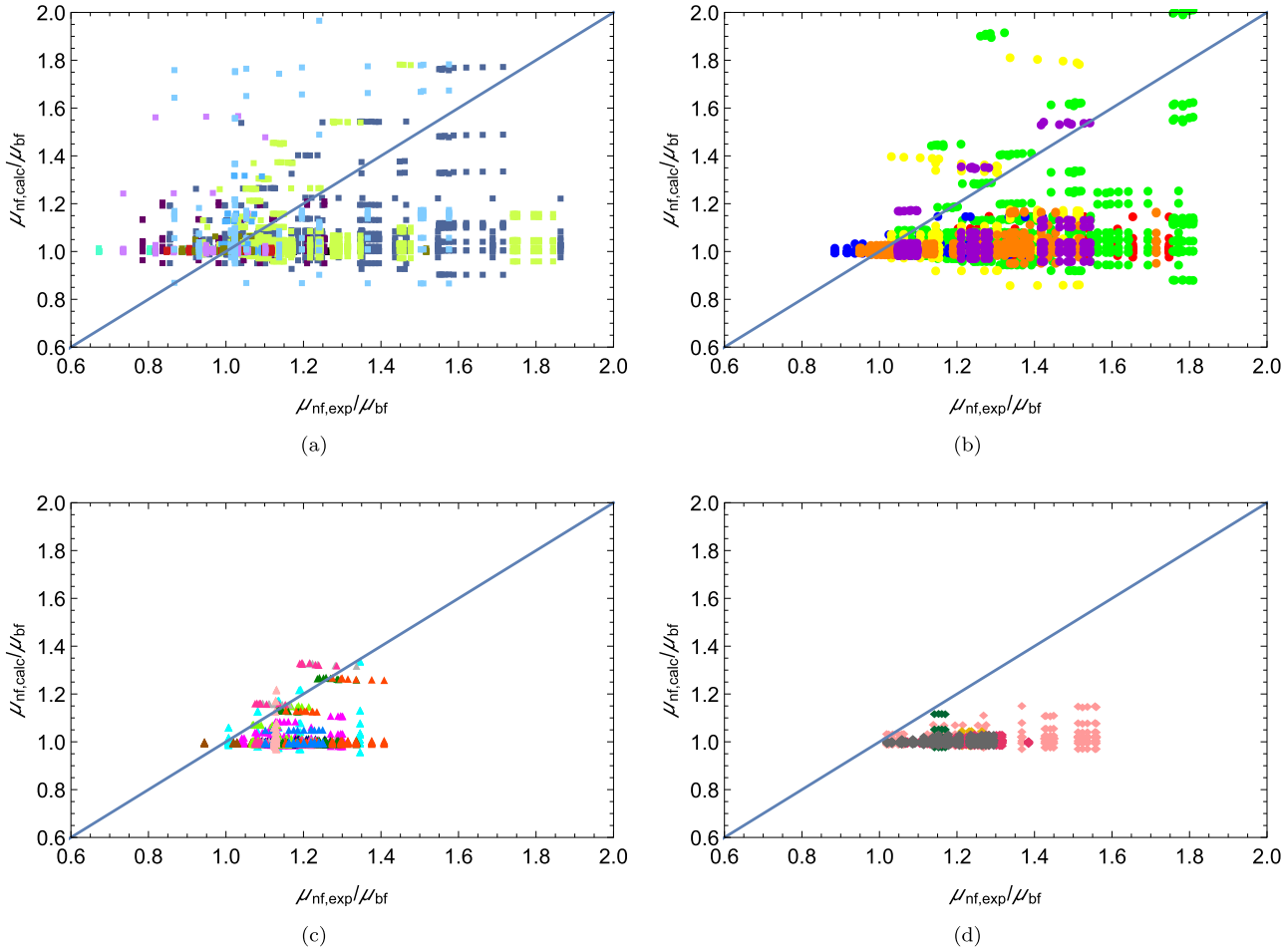

Fig. 4. Comparison of measured and predicted dynamic viscosity for water-based nanofluids (a), ethylene glycol-based nanofluids (b), mixtures of water and ethylene glycol nanofluids (c), and mixtures of water and propylene glycol nanofluids (d). The legend is the same of Fig. 1.

Table 8
AARD(μ_{nf}) (%) of the literature equations for water-based nanofluids.

Equation	Avg.	Ag	Al_2O_3	Al_2O_3-CuO	C	CuO	Diamond	Fe-Si	MWCNT	ND-Ni	TiO_2
Einstein [65] (1)	10.85	12.43	12.24	22.08	12.50	10.36	4.58	7.97	6.32	12. 74	7.28
Eilers [66] (2)	10.90	12.43	13.63	22.04	12.69	10.32	3.70	7.42	6.35	12.62	7.83
De Bruijn [67] (3)	11.99	12.45	17.73	21.96	13.76	10.87	3.98	7.54	6.43	12.34	12.86
Vand [68] (4)	10.76	12.43	12.11	22.08	12.48	10.36	4.58	7.37	6.32	12.74	7.16
Saitô [69] (5)	11.16	12.44	14.57	22.02	12.82	10.38	3.88	7.45	6.38	12.54	9.14
Brinkman [70] (6)	10.61	12.43	12.16	22.08	12.49	10.36	2.98	7.37	6.32	12.74	7.21
Krieger and Dougherty [71] (7)	11.04	12.44	14.51	22.02	12.82	10.38	2.78	7.45	6.38	12.54	9.04
Thomas [72] (8)	10.62	12.37	11.94	22.41	12.45	10.45	2.94	7.33	6.27	12.84	7.15
Nielsen [73] (9)	10.88	12.43	11.25	22.08	12.48	10.86	3.54	7.37	6.32	12.79	9.68
Lundgren [74] (10)	10.60	12.43	12.12	22.08	12.48	10.36	2.88	7.37	6.32	12.74	7.17
Batchelor [75] (11)	10.67	12.43	12.13	22.08	12.48	10.36	3.58	7.37	6.32	12.74	7.19
Maıga et al. [77] (12)	12.14	13.41	9.98	22.19	15.78	11.72	4.26	7.19	6.20	13.14	17.56
Guo et al. [78] (13)	40.87	12.37	40.32	23.68	158.74	27.07	12.97	7.24	6.59	49.12	70.55
Corcione [79] (14)	11.60	12.43	10.47	22.07	15.86	10.49	2.89	7.39	6.30	12.97	15.08
Proposed model (17)	10.56	10.35	10.15	21.15	15.94	11.24	2.26	7.15	6.05	15.04	6.23

6.1.3. Results for nanofluids based on mixtures of water and ethylene glycol

The analysis of the nanofluids having EG-H_2O mixtures as base fluid shows that the best model is Guo's (13), with an AARD(μ_{nf}) of 7.11%, as can be seen from Table 10, from which a good behavior can be also observed with the nanofluids EG-H_2O(20:80)+Al_2O_3 and EG-H_2O(50:50)+nD87 (AARD of 3.48% and 1.89%, respectively). The worst model is De Bruijin's (3), which has an average AARD(μ_{nf}) of 14.45% and shows the highest AARD values for each nanofluid. The remaining models predict dynamic viscosity quite similarly, with an average AARD(μ_{nf}) just above 13%. Fig. 4(c) shows that the nanofluids with mixtures of water and ethylene glycol are underestimated by the literature equations. The nanofluids EG-H_2O(20:80)+Al_2O_3, EG-H_2O(50:50)+nD87 and EG-H_2O(50:50)+Al_2O_3 are the most underestimated of the literature.

6.1.4. Results for propylene glycol-based nanofluids and water-propylene glycol mixtures

The analysis of the nanofluids having PG and PG-H_2O mixtures as base fluids shows that the best model is Maiga's (12), which has an

Table 9
AARD(μ_{nf}) (%) of the literature equations for ethylene glycol-based nanofluids.

Equation	Avg.	Ag	Al_2O_3	CeO_2	Co_3O_4	SiC	TiO_2-CuO
Einstein [65] (1)	17.38	23.86	21.35	12.57	13.74	14.90	17.86
Eilers [66] (2)	18.69	24.41	23.14	12.77	17.28	15.52	19.00
De Bruijn [67] (3)	21.72	25.66	27.27	13.22	25.54	16.99	21.61
Vand [68] (4)	17.35	23.84	21.13	12.57	13.91	14.86	17.80
Saitô [69] (5)	24.52	24.76	24.26	12.98	19.45	45.93	19.72
Brinkman [70] (6)	17.27	23.85	21.22	12.57	13.26	14.88	17.82
Krieger and Dougherty [71] (7)	19.47	24.75	24.16	12.89	19.30	15.92	19.81
Thomas [72] (8)	16.96	23.69	20.85	12.45	12.45	14.75	17.55
Nielsen [73] (9)	16.42	23.65	18.59	12.52	11.67	14.74	17.36
Lundgren [74] (10)	17.21	23.85	21.16	12.57	13.02	14.87	17.81
Batchelor [75] (11)	17.22	23.85	21.17	12.57	13.08	14.84	17.81
Maıga et al. [77] (12)	13.97	21.88	12.20	11.92	12.16	12.45	13.22
Guo et al. [78] (13)	19.46	17.45	24.55	8.95	47.09	11.32	7.39
Corcione [79] (14)	17.87	23.27	14.17	12.36	28.30	14.20	14.92
Proposed model (17)	9.63	18.10	5.14	9.58	9.69	8.14	7.11

Table 10
AARD(μ_{nf}) (%) of the literature equations for nanofluids based on mixtures of water and ethylene glycol.

EG-H_2O (wt%)		20:80	20:80	50:50	50:50	50:50	50:50	50:50	50:50	50:50	50:50	60:40
Equation	Avg.	Al_2O_3	MWCNT-WO_3	Al_2O_3	CB	fGnP	G/Dp	G/Dr	nD87	nD97	TiO2	Al_2O_3
Einstein [65] (1)	13.38	10.65	11.96	8.99	11.10	13.49	14.68	13.25	16.99	20.42	15.80	9.82
Eilers [66] (2)	13.70	11.68	12.34	9.04	11.37	13.72	14.85	13.43	17.13	20.56	15.86	10.72
De Bruijn [67] (3)	14.45	14.10	13.22	9.17	11.99	14.25	15.26	13.84	17.45	20.86	16.01	12.78
Vand [68] (4)	13.37	10.60	11.95	8.99	11.09	13.49	14.68	13.25	16.99	20.42	15.80	9.79
Saitô [69] (5)	13.91	12.35	12.59	9.08	11.54	13.87	14.97	13.54	17.22	20.64	15.90	11.29
Brinkman [70] (6)	13.47	10.62	11.95	8.99	11.10	13.49	14.68	13.25	16.99	20.42	15.80	9.80
Krieger and Dougherty [71] (7)	13.91	12.34	12.59	9.08	11.54	13.87	14.97	13.54	17.22	20.64	15.90	11.28
Thomas [72] (8)	13.14	10.45	11.71	8.79	10.85	13.25	14.44	13.01	16.76	20.19	15.57	9.53
Nielsen [73] (9)	13.29	10.48	11.77	8.99	11.03	13.44	14.63	13.20	16.96	20.39	15.80	9.50
Lundgren [74] (10)	13.37	10.61	11.95	8.99	11.10	13.49	14.68	13.25	16.99	20.42	15.80	9.79
Batchelor [75] (11)	13.37	10.61	11.95	8.99	11.10	13.49	14.68	13.25	16.99	20.42	15.80	9.79
Maıga et al. [77] (12)	12.25	7.05	10.63	8.81	10.19	12.73	14.10	12.66	16.53	19.98	15.60	6.42
Guo et al. [78] (13)	7.11	3.48	8.83	8.86	5.87	13.25	5.81	7.56	1.89	4.90	13.25	4.55
Corcione [79] (14)	13.02	9.20	11.74	9.02	10.82	13.68	14.37	12.94	16.78	20.22	15.77	8.66
Proposed model (17)	6.35	5.04	5.83	6.97	2.37	7.78	5.15	4.01	7.57	10.35	10.57	4.18

Table 11
AARD(μ_{nf}) (%) of the literature equations for propylene glycol-based nanofluids and water-propylene glycol mixtures.

PG-H_2O (wt%)		100:00	20:80	20:80	30:70	50:50
Equation	Avg.	SiC	TiB_2	TiB_2-B_4C	fGnP	fGnP
Einstein [65] (1)	15.72	18.95	18.18	11.99	16.51	12.95
Eilers [66] (2)	16.28	19.62	18.74	12.91	16.84	13.31
De Bruijn [67] (3)	17.59	21.15	20.02	15.02	17.60	14.15
Vand [68] (4)	15.69	18.92	18.16	11.95	16.50	12.94
Saitô [69] (5)	17.25	20.04	19.10	16.50	17.05	13.55
Brinkman [70] (6)	15.70	18.93	18.17	11.97	16.51	12.94
Krieger and Dougherty [71] (7)	16.65	20.04	19.09	13.50	17.05	13.55
Thomas [72] (8)	15.46	18.69	17.94	11.70	16.27	12.70
Nielsen [73] (9)	15.57	18.57	18.17	11.97	16.34	12.78
Lundgren [74] (10)	15.70	18.93	18.17	11.96	16.50	12.94
Batchelor [75] (11)	17.02	19.73	20.17	14.65	17.52	13.04
Maıga et al. [77] (12)	13.65	16.45	16.20	8.53	15.37	11.69
Guo et al. [78] (13)	57.48	13.50	243.05	2.95	15.78	12.14
Corcione [79] (14)	14.82	18.23	15.01	11.16	16.64	13.07
Proposed model (17)	5.37	8.69	1.97	6.37	4.82	5.01

average AARD(μ_{nf}) equal to 13.65%, as can be seen from Table 11. The same table shows how this result is affected by the AARD(μ_{nf}) of PG+SiC and PG-H_2O(20:80)+TiB_2, which are close to 16% error. Again, the Guo's model (13) is the worst because it presents an average AARD(μ_{nf}) of 57.48%. However, the result is strongly influenced by PG-H_2O(20:80)+TiB_2, for which it has an AARD of 243.05%. The models of Eilers (2), Saito (5), Krieger-Dougherty (7) and De Bruijin (3) have a very similar behavior, with an AARD(μ_{nf}) of more than 16.50%. While the models proposed by Einstein (1), Vand (4), Brinkman (6), Thomas (8), Nielsen (9), and Lundgren (10) produce very similar outcomes, with an AARD(μ_{nf}) of around 15.50%. Table 11 indicates that all models have an AARD(μ_{nf}) of over 10%, except for the nanofluid PG-H_2O(20:80)+TiB_2-B_4C. In this case, Maiga's (12) and Guo's (13) models yield an AARD(μ_{nf}) of 8.53% and 2.95%, respectively. Fig. 4(d) shows how the equations in the literature tend to underestimate all nanofluids with mixtures of water and propylene glycol as base fluids.

6.2. Results for the proposed correlation

Fig. 3 illustrates that the literature equations often underestimate μ_{nf}. Specifically, De Bruijin's, Krieger-Dougherty's, Thomas's, and Batchelor's models (Eqs. (3), (7), (8), and (11)) are notable for this ten-

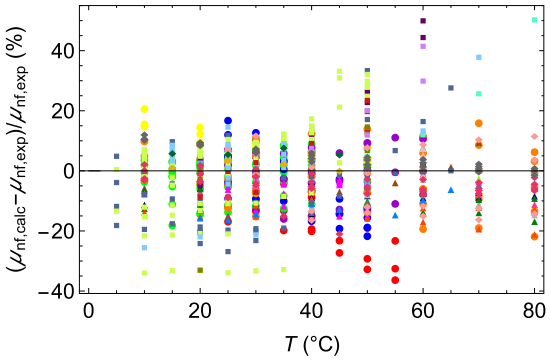

Fig. 5. Temperature-dependent deviations in dynamic viscosity according to Eq. (17). The legend is the same of Fig. 1.

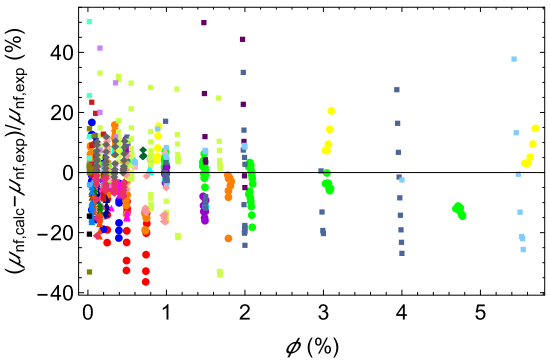

Fig. 6. Nanoparticle-volume-concentration-dependent deviations in dynamic viscosity according to Eq. (17). The legend is the same of Fig. 1.

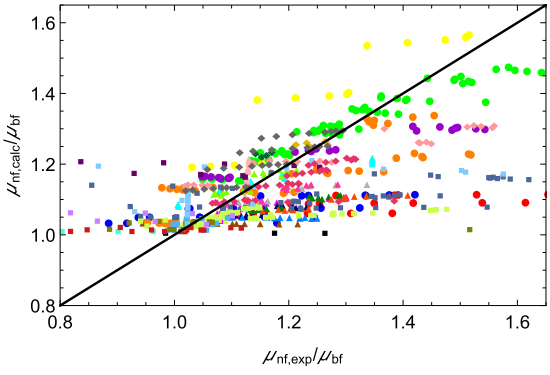

Fig. 7. Experimental reduced dynamic viscosity vs. calculated values for Eq. (17). The legend is the same of Fig. 1.

dency. In contrast, Maiga and Guo's models (Eqs (12) and (13)) tend to overestimate the dynamic viscosity calculation.

The results of the proposed correlation (Eq. (17)) are provided in Table 7, 8, 9, 10, 11, and in Fig. 5, 6 and 7. In Fig. 5, it can be seen that the relative error does not exhibit a discernible correlation with temperature, indicating that the model accuracy remains relatively consistent across the entire temperature range under consideration. This observation is further supported by the results presented in Fig. 6, but demonstrates that higher concentrations yield to higher errors. This phenomenon, in part, depends on the limited availability of data at high volumetric concentrations, which in turn affects the precision of the resulting estimates at these concentrations. Fig. 7 shows how the proposed model slightly underestimates some nanofluids, such as H_2O+CuO and H_2O+Al_2O_3, while slightly overestimates others, such as PG-H_2O(50:50) +fGnP, EG+Co_3O_4, and PG+SiC.

Table 12
AARD(μ_{nf}) (%) for the 4-fold cross-validation used on Eq. (17).

Test	Regressed Dataset %	Predicted Dataset %	Complete Dataset %
1	8.04	8.18	8.23
2	7.41	8.18	8.44
3	9.15	8.15	7.82
4	8.23	8.18	8.16

As can be seen from Table 7, the suggested model exhibits an overall average AARD(μ_{nf}) of 8.16% across the entire dataset, result that is significantly better with respect to the average AARD(μ_{nf}) value related to all the literature equations (14.66%). The consideration is also true if the proposed correlation is compared with Maiga's model (12), which provides the best AARD(μ_{nf}) among the equations available in the literature (12.33%).

Studying the results for the nanofluids that have H_2O as base fluid (Table 8), it can be seen that the proposed model shows an average AARD(μ_{nf}) of 10.56%, a result then is slightly better with respect of what can be obtained with the literature equations. From Table 8, it can be seen that the proposed model has low AARD(μ_{nf}) values for the nanofluids H_2O+Diamond, H_2O+MWCNT and H_2O+Fe-Si (2.26%, 6.05% and 7.15%, respectively). However, it has poor compatibility with H_2O+Al_2O_3/CuO and H_2O+C nanofluids, for which the AARD(μ_{nf}) is 21.15% and 15.94%, respectively. For these nanofluids, however, the proposed model presents AARD(μ_{nf}) values in line with the literature.

From Table 9, where the results for nanofluids having ethylene glycol (EG) as base fluid are detailed, it can be seen that the proposed model has an average AARD(μ_{nf}) of 9.63%, while the literature equations exhibit an average AARD(μ_{nf}) exceeding 15%. This is due to a very good compatibility displayed by the model with EG+Al_2O_3 (AARD(μ_{nf}) of 5.14%), EG+TiO_2/CuO (AARD(μ_{nf}) of 7.11%), and EG+SiC (AARD(μ_{nf}) of 8.14%). But the AARD(μ_{nf}) related to EG+Ag nanofluid, which is 18.1%, negatively impacts the overall result.

Studying the results for the nanofluids having mixtures of EG-H_2O as base fluid (Table 10), it can be seen that the proposed model presents an average AARD(μ_{nf}) of 6.35%. It also exhibits AARD(μ_{nf}) values of less than 6% for various nanofluids such as EG-H_2O(20:80)+Al_2O_3, EG-H_2O(20:80)+MWCNT/WO_3, EG-H_2O(50:50)+CB (nanofluid for which it also exhibits the lowest AARD(μ_{nf}) value of 2.37%), EG-H_2O(50:50)+G/Dp and EG-H_2O(60:40)+Al_2O_3. These deviations show that the model exhibits better behavior with respect to the literature equations, apart from a few exceptions where Guo's model (13) gives slightly better results.

From Table 11, where results are presented for nanofluids having propylene glycol (PG) and mixtures of propylene glycol and water (PG-H_2O) as base fluid, it can be seen that the proposed model exhibits an average AARD(μ_{nf}) of 5.37%. The proposed model presents very low AARD(μ_{nf}) values for all the considered nanofluids, particularly for PG-H_2O(30:70)+fGnP and PG-H_2O(20:80)+TiB_2, for which the AARD(μ_{nf}) is 4.82% and 1.97%, respectively.

The efficacy of the suggested model was evaluated through the implementation of a k-fold cross-validation technique, which was utilized to assess its capacity for generalization. In the k-fold cross-validation method, the dataset is divided into k equal parts. For model coefficient estimation, $k-1$ of these subsets are used, while the leftover subset evaluates the model's ability to predict outcomes. This procedure iterates k times, cycling through all subsets. In conducting their analysis, the study's authors employed a fourfold cross-validation approach. Table 12 presents the findings of each test. The high generalization capability of the proposed Eq. (17) is demonstrated by the obtained deviations.

Finally, Fig. 8 shows the temperature dependence of the proposed Eq. (17) for five nanofluid samples selected from the dataset, provided with their experimental values. It can be seen that the proposed correlation effectively captures the physical progression of dynamic viscosity as function of temperature.

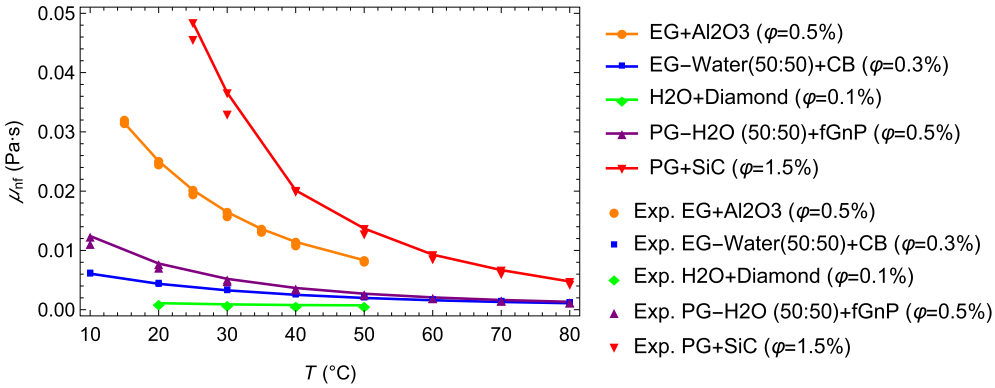

Fig. 8. Trend of the proposed Eq. (17) with temperature for different nanofluids. The symbols represent the experimental values.

Table 13
Average AARD(μ_{nf}) (%) of the literature equations regressed on the database.

	Avg. AARD(μ_{nf}) (%)	Eq.
Einstein [65]	11.52	(1)
Eilers [66]	11.58	(2)
De Bruijn [67]	10.90	(3)
Vand [68]	10.97	(4)
Saitô [69]	13.66	(5)
Brinkman [70]	11.92	(6)
Krieger and Dougherty [71]	12.62	(7)
Thomas [72]	10.34	(8)
Nielsen [73]	11.70	(9)
Lundgren [74]	12.30	(10)
Batchelor [75]	10.90	(11)
Maiga et al. [77]	10.90	(12)
Guo et al. [78]	11.48	(13)
Corcione [79]	10.30	(14)

6.3. Results for literature equations regressed on database

As discussed in Section 5, the 14 selected literature equations were regressed on the database in order to obtain new coefficients that would reduce the error committed by the original formulations. Table 13 shows the AARD(μ_{nf}) values of the literature equations after this re-fitting operation. After comparing these results with those in Table 7, it appears that all models show a marked improvement. The equation that mostly benefits from the operation is that of Corcione (14), which reaches an average AARD(μ_{nf}) of 10.30%. Despite this, the proposed Eq. (17) still provides more accurate predictions (AARD(μ_{nf}) of 8.16%) than the re-fitted literature equations.

7. Conclusions

In order to evaluate the precision of several renowned correlations pertaining to the dynamic viscosity of nanofluids (μ_{nf}), an experimental dataset of 737 points and 32 different nanofluids was collected in this work. The study examined and assessed a total of 14 correlations and a semi-empirical scaled equation proposed by the authors.

Based on the results of the study, the main findings can be summarized as follows.

- For the entire dataset, the best literature equation is Maiga's [77] (AARD(μ_{nf}) = 12.33%).
- For H_2O-based nanofluids, the best literature model is Lundgren's [74] (AARD(μ_{nf}) = 10.60%).
- For EG-based nanofluids, the best literature equation is Maiga's [77] (AARD(μ_{nf}) = 13.97%).
- For base fluids consisting of mixtures of H_2O and EG, the best literature model is Guo's [78] (AARD(μ_{nf}) = 7.11%).
- For base fluids consisting of mixtures of H_2O and PG, the best literature model is Maiga's [77] (AARD(μ_{nf}) = 13.65%).
- Applying the Random Search Method (RSM) to the literature equations, it was found that the best re-fitted model was the one of Corcione (14) (AARD(μ_{nf}) = 10.30%).
- The correlation proposed by the authors (Eq. (17)) was found to have an AARD(μ_{nf}) = 8.16% for the entire dataset. The correlation also showed the best results for each sub-group of the base fluids. A 4-fold cross validation proved its generalization capability with new data.

In conclusion, it is recommended that researchers provide comprehensive descriptions of the methodologies employed in the preparation of nanofluids, including detailed numerical data, instruments, zeta potential, and pH values utilized.

CRediT authorship contribution statement

Gianluca Coccia: Writing – review & editing, Writing – original draft, Supervision, Methodology, Conceptualization. **Feliciano Falcone:** Writing – review & editing, Writing – original draft, Validation, Investigation, Data curation.

Declaration of competing interest

The authors declare that they have no known competing financial interests or personal relationships that could have appeared to influence the work reported in this paper.

Data availability

Data will be made available on request.

References

[1] S.K. Das, S.U. Choi, W. Yu, T. Pradeep, Nanofluids: Science and Technology, John Wiley & Sons, 2007.
[2] J.C. Maxwell, A Treatise on Electricity and Magnetism, vol. 1, Clarendon Press, 1873.
[3] P. Nagarajan, J. Subramani, S. Suyambazhahan, R. Sathyamurthy, Nanofluids for solar collector applications: a review, Energy Proc. 61 (2014) 2416–2434.
[4] C. Bobbo Fedele, Nanofluidi Come Fluidi di Nuova Generazione Ad Elevata Efficienza, Università degli Studi di Padova, 2011.
[5] W. Yu, H. Xie, A review on nanofluids: preparation, stability mechanisms, and applications, J. Nanomater. 2012 (2012) 1–17.
[6] N. Sezer, M.A. Atieh, M. Koç, A comprehensive review on synthesis, stability, thermophysical properties, and characterization of nanofluids, Powder Technol. 344 (2019) 404–431.
[7] Enhancing the Performance of Parabolic Trough Collectors Using Nanofluids and Turbulators, Renew. Sustain. Energy Rev. 91 (2018) 358–375, https://doi.org/10.1016/j.rser.2018.03.091.
[8] D. Zheng, J. Du, W. Wang, J.J. Klemeš, J. Wang, B. Sundén, Analysis of thermal efficiency of a corrugated double-tube heat exchanger with nanofluids, Energy 256 (2022) 124522.

[9] W. Ajeeb, R.R.T. da Silva, S.S. Murshed, Experimental investigation of heat transfer performance of al2o3 nanofluids in a compact plate heat exchanger, Appl. Therm. Eng. 218 (2023) 119321.
[10] V. Ghazanfari, M. Imani, M.M. Shadman, Y. Amini, F. Zahakifar, Numerical study on the thermal performance of the shell and tube heat exchanger using twisted tubes and al2o3 nanoparticles, Prog. Nucl. Energy 155 (2023) 104526.
[11] P.M.J. Stalin, T.V. Arjunan, M. Almeshaal, P. Murugesan, B. Prabu, P.M. Kumar, Utilization of zinc-ferrite/water hybrid nanofluids on thermal performance of a flat plate solar collector—a thermal modeling approach, Environ. Sci. Pollut. Res. 29 (2022) 78848–78861.
[12] J. Mustafa, S. Alqaed, M. Sharifpur, Evaluation of energy efficiency, visualized energy, and production of environmental pollutants of a solar flat plate collector containing hybrid nanofluid, Sustain. Energy Technol. Assessments 53 (2022) 102399.
[13] S.M. Henein, A.A. Abdel-Rehim, K. El-Nagar, Energy, economic and environmental analysis of an evacuated tube solar collector using hybrid nanofluid, Appl. Therm. Eng. 219 (2023) 119671.
[14] B.V. Balakin, M. Stava, A. Kosinska, Photothermal convection of a magnetic nanofluid in a direct absorption solar collector, Sol. Energy 239 (2022) 33–39.
[15] A. Joseph, S. Thomas, Energy, exergy and corrosion analysis of direct absorption solar collector employed with ultra-high stable carbon quantum dot nanofluid, Renew. Energy 181 (2022) 725–737.
[16] G. Coccia, G. Di Nicola, S. Tomassetti, M. Pierantozzi, G. Passerini, Determination of the Boyle temperature of pure gases using artificial neural networks, Fluid Phase Equilib. 493 (2019) 36–42.
[17] S. Tomassetti, G. Coccia, M. Pierantozzi, G. Di Nicola, Correlations for liquid thermal conductivity of low gwp refrigerants in the reduced temperature range 0.4 to 0.9 from saturation line to 70 mpa, Int. J. Refrig. 117 (2020) 358–368.
[18] A.D. Zadeh, D. Toghraie, Experimental investigation for developing a new model for the dynamic viscosity of silver/ethylene glycol nanofluid at different temperatures and solid volume fractions, J. Therm. Anal. Calorim. 131 (2018) 1449–1461.
[19] M.J. Pastoriza-Gallego, L. Lugo, J.L. Legido, M.M. Piñeiro, Thermal conductivity and viscosity measurements of ethylene glycol-based al 2 o 3 nanofluids, Nanoscale Res. Lett. 6 (2011) 1–11.
[20] A.H. Saeedi, M. Akbari, D. Toghraie, An experimental study on rheological behavior of a nanofluid containing oxide nanoparticle and proposing a new correlation, Physica E, Low-Dimens. Syst. Nanostruct. 99 (2018) 285–293.
[21] A. Mariano, M.J. Pastoriza-Gallego, L. Lugo, L. Mussari, M.M. Piñeiro, Co3o4 ethylene glycol-based nanofluids: thermal conductivity, viscosity and high pressure density, Int. J. Heat Mass Transf. 85 (2015) 54–60.
[22] S. Akilu, A.T. Baheta, K. Kadirgama, E. Padmanabhan, K. Sharma, Viscosity, electrical and thermal conductivities of ethylene and propylene glycol-based β-sic nanofluids, J. Mol. Liq. 284 (2019) 780–792.
[23] L. Colla, Experimental characterization of nanofluids as heat transfer media, 2014.
[24] S. Akilu, A.T. Baheta, K. Sharma, Experimental measurements of thermal conductivity and viscosity of ethylene glycol-based hybrid nanofluid with tio2-cuo/c inclusions, J. Mol. Liq. 246 (2017) 396–405, https://doi.org/10.1016/j.molliq.2017.09.017.
[25] L.S. Sundar, E.V. Ramana, M.K. Singh, A.C. Sousa, Thermal conductivity and viscosity of stabilized ethylene glycol and water mixture al2o3 nanofluids for heat transfer applications: an experimental study, Int. Commun. Heat Mass Transf. 56 (2014) 86–95.
[26] T. Yiamsawas, O. Mahian, A.S. Dalkilic, S. Kaewnai, S. Wongwises, Experimental studies on the viscosity of tio2 and al2o3 nanoparticles suspended in a mixture of ethylene glycol and water for high temperature applications, Appl. Energy 111 (2013) 40–45.
[27] Y. Zhu, M. Zamani, G. Xu, D. Toghraie, M. Hashemian, A.a. Alizadeh, A comprehensive experimental investigation of dynamic viscosity of mwcnt-wo3/water-ethylene glycol antifreeze hybrid nanofluid, J. Mol. Liq. 333 (2021) 115986.
[28] Z. Said, M.A. Abdelkareem, H. Rezk, A.M. Nassef, Fuzzy modeling and optimization for experimental thermophysical properties of water and ethylene glycol mixture for al2o3 and tio2 based nanofluids, Powder Technol. 353 (2019) 345–358.
[29] J.P. Vallejo, G. Żyła, J. Fernández-Seara, L. Lugo, Influence of six carbon-based nanomaterials on the rheological properties of nanofluids, Nanomaterials 9 (2019) 146.
[30] H. Khosravi-Bizhaem, A. Abbassi, M.R. Salimpour, A. Zivari-Ravan, Experimental study on heat transfer, entropy generation, and exergy destruction of ag, mwcnt, and go water-based nanofluids in helical tubes, J. Therm. Anal. Calorim. (2022) 1–24.
[31] E.B. Elcioglu, A.G. Yazicioglu, A. Turgut, A.S. Anagun, Experimental study and Taguchi analysis on alumina-water nanofluid viscosity, Appl. Therm. Eng. 128 (2018) 973–981.
[32] V. Nair, A. Parekh, P. Tailor, Experimental investigation of thermophysical properties of r718 based nanofluids at low temperatures, Heat Mass Transf. 55 (2019) 2769–2784.
[33] G. Coccia, G. Di Nicola, L. Colla, L. Fedele, M. Scattolini, Adoption of nanofluids in low-enthalpy parabolic trough solar collectors: numerical simulation of the yearly yield, Energy Convers. Manag. 118 (2016) 306–319.
[34] C. Nguyen, F. Desgranges, G. Roy, N. Galanis, T. Maré, e. Boucher, H.A. Mintsa, Temperature and particle-size dependent viscosity data for water-based nanofluids–hysteresis phenomenon, Int. J. Heat Fluid Flow 28 (2007) 1492–1506.
[35] M. Zufar, P. Gunnasegaran, H. Kumar, K. Ng, Numerical and experimental investigations of hybrid nanofluids on pulsating heat pipe performance, Int. J. Heat Mass Transf. 146 (2020) 118887.
[36] A. Dalkilic, A. Çebi, A. Celen, O. Yıldız, O. Acikgoz, C. Jumpholkul, M. Bayrak, K. Surana, S. Wongwises, Prediction of graphite nanofluids' dynamic viscosity by means of artificial neural networks, Int. Commun. Heat Mass Transf. 73 (2016) 33–42.
[37] M.J. Pastoriza-Gallego, C. Casanova, J.a. Legido, M.M. Piñeiro, Cuo in water nanofluid: influence of particle size and polydispersity on volumetric behaviour and viscosity, Fluid Phase Equilib. 300 (2011) 188–196.
[38] A.A. Alrashed, M.S. Gharibdousti, M. Goodarzi, L.R. de Oliveira, M.R. Safaei, E.P. Bandarra Filho, Effects on thermophysical properties of carbon based nanofluids: experimental data, modelling using regression, anfis and ann, Int. J. Heat Mass Transf. 125 (2018) 920–932.
[39] G. Huminic, A. Huminic, C. Fleacă, F. Dumitrache, I. Morjan, Experimental study on viscosity of water based fe–si hybrid nanofluids, J. Mol. Liq. 321 (2021) 114938.
[40] L.S. Sundar, M.K. Singh, A.C. Sousa, Turbulent heat transfer and friction factor of nanodiamond-nickel hybrid nanofluids flow in a tube: an experimental study, Int. J. Heat Mass Transf. 117 (2018) 223–234.
[41] W. Duangthongsuk, S. Wongwises, Measurement of temperature-dependent thermal conductivity and viscosity of tio2-water nanofluids, experimental thermal and fluid, Science 33 (2009) 706–714.
[42] G.J. Tertsinidou, C.M. Tsolakidou, M. Pantzali, M.J. Assael, L. Colla, L. Fedele, S. Bobbo, W.A. Wakeham, New measurements of the apparent thermal conductivity of nanofluids and investigation of their heat transfer capabilities, J. Chem. Eng. Data 62 (2017) 491–507.
[43] L. Fedele, L. Colla, S. Bobbo, Viscosity and thermal conductivity measurements of water-based nanofluids containing titanium oxide nanoparticles, Int. J. Refrig. 35 (2012) 1359–1366.
[44] J.P. Vallejo, G. Żyła, L. Ansia, J. Fal, J. Traciak, L. Lugo, Thermophysical, rheological and electrical properties of mono and hybrid tib2/b4c nanofluids based on a propylene glycol: water mixture, Powder Technol. 395 (2022) 391–399.
[45] J.P. Vallejo, G. Żyła, J. Fernández-Seara, L. Lugo, Rheological behaviour of functionalized graphene nanoplatelet nanofluids based on water and propylene glycol: water mixtures, Int. Commun. Heat Mass Transf. 99 (2018) 43–53.
[46] J. Pérez-Tavernier, J. Vallejo, D. Cabaleiro, J. Fernández-Seara, L. Lugo, Heat transfer performance of a nano-enhanced propylene glycol: water mixture, Int. J. Therm. Sci. 139 (2019) 413–423.
[47] J. Zhu, D. Li, H. Chen, X. Yang, L. Lu, X. Wang, Highly dispersed cuo nanoparticles prepared by a novel quick-precipitation method, Mater. Lett. 58 (2004) 3324–3327.
[48] U. Westhaus, T. Dröge, R. Sass, Detherm®—a thermophysical property database, Fluid Phase Equilib. 158 (1999) 429–435.
[49] C.S. Cragoe, Aroperties of ethylene glycol and its aqueous solutions, report of the cooperative fuel research committee of the coordinating, 1943.
[50] Y.A. Çengel, R.H. Turner, J.M. Cimbala, M. Kanoglu, Fundamentals of Thermal-Fluid Sciences, vol. 703, McGraw-Hill, New York, 2001.
[51] S. Akilu, A.T. Baheta, K. Kadirgama, E. Padmanabhan, K. Sharma, Viscosity, electrical and thermal conductivities of ethylene and propylene glycol-based β-sic nanofluids, J. Mol. Liq. 284 (2019) 780–792.
[52] P. Baraldi, G.C. Franchini, A. Marchetti, G. Sanna, L. Tassi, A. Ulrici, G. Vaccari, Density and volume properties of ethane-1, 2-diol+ 1, 2-dimethoxyethane+ water ternary mixtures from- 10° to 80°, J. Solution Chem. 29 (2000) 489–504.
[53] T. Sun, A.S. Teja, Density, viscosity and thermal conductivity of aqueous solutions of propylene glycol, dipropylene glycol, and tripropylene glycol between 290 k and 460 k, J. Chem. Eng. Data 49 (2004) 1311–1317.
[54] A.H. Ashrae, Fundamentals, si ed, American Society of Heating, Refrigerating and Air-Conditioning Engineers, Atlanta, GA, 2017.
[55] T.K. Sherwood, R.C. Reid, The Properties of Gases and Liquids: Their Estimation and Correlation, McGraw-Hill, 1958.
[56] P.T. Yurkevich, D. Komarov, Influence of quantity and character of filling material on thermophysical properties of composite sorbent materials for a thermocompressor, Russ. J. Appl. Chem. (1995).
[57] J. Gmehling, J. Krafczyk, J. Ahlers, S. Nebig, I. Hunecker, M. Eisel, D. Fischer, B. Krentscher, K. Beyer, Pure Compound Data from ddb, Dortmund Data Bank 2014, 1983.
[58] L.S. Sundar, E.V. Ramana, M.K. Singh, A.C. Sousa, Thermal conductivity and viscosity of stabilized ethylene glycol and water mixture al2o3 nanofluids for heat transfer applications: an experimental study, Int. Commun. Heat Mass Transf. 56 (2014) 86–95.
[59] L.S. Sundar, K. Sharma, M. Naik, M.K. Singh, Empirical and theoretical correlations on viscosity of nanofluids: a review, Renew. Sustain. Energy Rev. 25 (2013) 670–686.
[60] K. Bashirnezhad, S. Bazri, M.R. Safaei, M. Goodarzi, M. Dahari, O. Mahian, A.S. Dalkılıça, S. Wongwises, Viscosity of nanofluids: a review of recent experimental studies, Int. Commun. Heat Mass Transf. 73 (2016) 114–123.
[61] A. Patra, M. Nayak, A. Misra, Viscosity of nanofluids-a review, Int. J. Thermofluid Sci. Technol. 7 (2020) 070202.
[62] J.P. Meyer, S.A. Adio, M. Sharifpur, P.N. Nwosu, The viscosity of nanofluids: a review of the theoretical, empirical, and numerical models, Heat Transf. Eng. 37 (2016) 387–421.
[63] H.D. Koca, S. Doganay, A. Turgut, I.H. Tavman, R. Saidur, I.M. Mahbubul, Effect of particle size on the viscosity of nanofluids: a review, Renew. Sustain. Energy Rev. 82 (2018) 1664–1674.

[64] A. Patra, M. Nayak, A. Misra, Viscosity of nanofluids-a review, Int. J. Thermofluid Sci. Technol. 7 (2020) 070202.
[65] A. Einstein, Eine neue bestimmung der molekuldimensionen, Ann. Phys. 34 (1911) 591–592.
[66] v.H. Eilers, Die viskosität von emulsionen hochviskoser stoffe als funktion der konzentration, Kolloid-Zeitschrift 97 (1941) 313–321.
[67] H. De Bruijn, The viscosity of suspensions of spherical particles. (the fundamental η-c and φ relations), Recueil des Travaux Chimiques des Pays-Bas 61 (1942) 863–874.
[68] V. Vand, Theory of viscosity of concentrated suspensions, Nature 155 (1945) 364–365.
[69] N. Saitô, Concentration dependence of the viscosity of high polymer solutions. i, J. Phys. Soc. Jpn. 5 (1950) 4–8.
[70] H.C. Brinkman, The viscosity of concentrated suspensions and solutions, J. Chem. Phys. 20 (1952) 571.
[71] I.M. Krieger, T.J. Dougherty, A mechanism for non-Newtonian flow in suspensions of rigid spheres, Trans. Soc. Rheol. 3 (1959) 137–152.
[72] D.G. Thomas, Transport characteristics of suspension: viii. A note on the viscosity of Newtonian suspensions of uniform spherical particles, J. Colloid Sci. 20 (1965) 267–277.
[73] L.E. Nielsen, Generalized equation for the elastic moduli of composite materials, J. Appl. Phys. 41 (1970) 4626–4627.
[74] T.S. Lundgren, Slow flow through stationary random beds and suspensions of spheres, J. Fluid Mech. 51 (1972) 273–299.
[75] G. Batchelor, The effect of Brownian motion on the bulk stress in a suspension of spherical particles, J. Fluid Mech. 83 (1977) 97–117.
[76] X. Wang, X. Xu, S.U. Choi, Thermal conductivity of nanoparticle-fluid mixture, J. Thermophys. Heat Transf. 13 (1999) 474–480.
[77] S.E.B. Maıga, C.T. Nguyen, N. Galanis, G. Roy, Heat transfer behaviours of nanofluids in a uniformly heated tube, Superlattices Microstruct. 35 (2004) 543–557.
[78] S. Guo, Z. Luo, T. Wang, J. Zhao, K. Cen, Viscosity of monodisperse silica nanofluids, Bull. Chin. Ceram. Soc. 25 (2006) 52–55.
[79] M. Corcione, Empirical correlating equations for predicting the effective thermal conductivity and dynamic viscosity of nanofluids, Energy Convers. Manag. 52 (2011) 789–793.
[80] A. Turco, Factor analysis usage and interpretation, Technical Report, ESTECO, 2011.
[81] T. Rietveld, R. van Hout, Statistical Techniques for the Study of Language and Language Behaviour, Mouton de Gruyter, New York, 1993.
[82] G. Coccia, S. Tomassetti, G. Di Nicola, Thermal conductivity of nanofluids: a review of the existing correlations and a scaled semi-empirical equation, Renew. Sustain. Energy Rev. 151 (2021) 111573.
[83] S. Andradóttir, An overview of simulation optimization via random search, Handb. Oper. Res. Manag. Sci. 13 (2006) 617–631.